Interfacial Catalysis by Phospholipase A_2: Determination of the Interfacial Kinetic Rate Constants†

Otto G. Berg,*,‡ Bao-Zhu Yu,§ Joe Rogers,§ and Mahendra Kumar Jain*,§

Department of Molecular Biology, Uppsala University Biomedical Center, Uppsala, Sweden, and Department of Chemistry, University of Delaware, Newark, Delaware 19716

Received September 17, 1990; Revised Manuscript Received March 26, 1991

ABSTRACT: Hydrolysis of vesicles of 1,2-dimyristoyl-*sn*-glycero-3-phosphomethanol (DMPM) by pig pancreatic phospholipase A_2 (PLA2) occurs in a highly processive "scooting" mode, and the rate is comparable to or exceeds the rates observed with detergent-dispersed mixed micelles under optimal conditions. A complete kinetic description of the steady-state time course of the hydrolysis is developed. The analysis covers the whole Michaelis–Menten space: it emphasizes the key features of interfacial catalysis by a detailed theoretical analysis, describes the experimental protocols to determine the values of the kinetic and equilibrium constants for interfacial catalysis, and provides an interpretation of the effect of calcium, substrate, products, apparent activators, and competitive inhibitors on the reaction progress curve by a single set of rate and equilibrium parameters. In this paper, the integrated reaction progress curve was rigorously interpreted in terms of a minimal model involving the Michaelis–Menten reaction sequence in the interface: $E^* + S \rightleftharpoons E^*S \rightarrow E^*P \rightleftharpoons E^* + P$, and most of the individual rate and equilibrium constants for the catalytic cycle were determined. This rigorous description of interfacial catalysis was made experimentally possible by examining the action of PLA2 in the scooting mode under conditions of at most one enzyme per vesicle, where it hydrolyzed all of the substrate in the outer monolayer of vesicles without leaving the surface. Other experimentally verified constraints for this analysis include the following: all enzyme was bound to vesicles; the integrity of vesicles was maintained during the course of hydrolysis; and the substrate, enzyme, and products did not exchange between vesicles nor did they exchange across the bilayer. The mechanistic significance of the rate constants is discussed in the accompanying papers.

Phospholipase A_2 (PLA2)[1] has attracted considerable attention because the mobilization and release of arachidonate and lysophospholipids from phospholipids in membranes is believed to be the rate-limiting step in the biosynthesis of eicosanoids and platelet-activating factor (Irvine, 1982; Burch, 1989). These compounds exhibit a wide range of physiological and pharmacological effects (Gallin et al., 1988). Since phospholipids in a cell are always present in interfaces, lipolytic enzymes such as PLA2s have evolved to be considerably more active at lipid–water interfaces, and their overall catalytic behavior is regulated by the organization and dynamics of the interface (Jain, 1972; Verger & de Haas, 1976; Verheij et al., 1981; Dennis, 1983; Jain & Berg, 1989). Such features of interfacial catalysis make it an intriguing biophysical phenomenon, and a full description of the underlying kinetic mechanism is a challenging undertaking because the overall process consists of the events associated with the catalytic cycle at the interface, and the interfacial binding step regulates the concentration of the enzyme at the interface.

Earlier (Jain et al., 1986a–d; Jain & Berg, 1989) we characterized the action of PLA2 on small vesicles of DMPM. This permitted a successful dissection of the contribution of the interfacial binding step from the catalytic steps in the interface according to the minimal model shown in Figure 1. Here PLA2 in the aqueous phase (E) binds to the interface, and the bound enzyme (E*) forms the Michaelis complex E*S, which undergoes catalytic change to E*P followed by dissociation to E* and the products. This scheme integrates the well-established Michaelis–Menten formalism (Fersht, 1985; Jencks, 1969; Segel, 1977) with a step in which the enzyme binds to the interface. It was first elaborated by Verger and de Haas (1976), and it has been invoked in several different forms to account for the dramatic increase in the rate of lipolysis at interfaces, such as monolayers (Verger et al., 1973), bilayers (Jain & Cordes, 1973), micelles (de Haas et al., 1971), and mixed-micelles (Dennis, 1973a,b).

Figure 1 is deceptively simple. In order to study the key features of interfacial catalysis, it is necessary to eliminate, constrain, or at least explicitly consider the parallel kinetic processes that could influence the overall rate of catalytic turnover (Jain & Berg, 1989). For example, as considered in Figure 2, if the enzyme hops from vesicle to vesicle during the catalytic turnover cycle, the rate of desorption and adsorption of the enzyme from the interface will be a part of the overall rate of catalytic turnover, i.e., the rate constants k_b and k_d will complicate the analysis of the interfacial rate processes. When the binding of the enzyme to the vesicle is tight, a processive reaction occurs in which thousands of catalytic cycles take place with the enzyme remaining bound to the same vesicle. This is referred to as hydrolysis in the scooting mode (Figure 2). The advantage of studying the catalysis in the highly processive scooting mode is that the E to E* step is not a part of the steps for the steady-state catalytic turnover within the interface. Thus, the hydrolysis of all the substrate molecules present in the outer monolayer of vesicles occurs processively in the scooting mode, as the enzyme does not leave the interface between the catalytic turnover cycles, and the overall rate of hydrolysis is not influenced by the absorption and desorption of the enzyme from the interface in between

† This work was supported by the NIH (GM29702) and Sterling Inc.
* To whom correspondence should be addressed.
‡ Uppsala University Biomedical Center.
§ University of Delaware.

[1] Abbreviations: DMPM, 1,2-dimyristoyl-*sn*-glycero-3-phosphomethanol; DTPM, 1,2-ditetradecyl-*sn*-glycero-3-phosphomethanol; PLA2, phospholipase A_2 from pig pancreas.

0006-2960/91/0430-7283$02.50/0

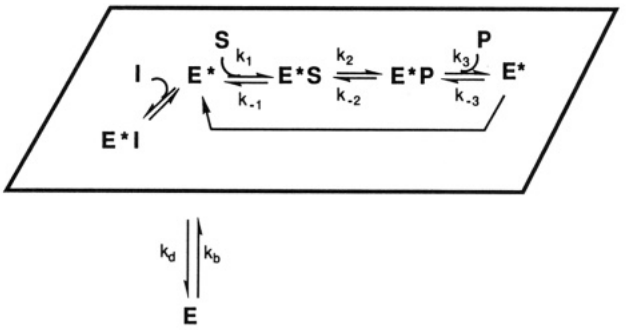

FIGURE 1: Scheme to accommodate key features of interfacial catalysis by PLA2. The species (E*, enzyme; I, inhibitor; S, substrate; P, products) shown in the box plane are in or bound to the bilayer, and the enzyme in the aqueous phase is shown as E. During the steady state, E is in equilibrium with the enzyme in the interface (E*), where according to the Michaelis–Menten formalism, E* brings about catalytic turnover by the steps shown in the box. Factors that regulate catalysis would modulate the steps in the box, while a shift in the E to E* equilibrium would modulate the apparent rate of catalytic turnover by increasing or decreasing the fraction of the total enzyme in the catalytically active E* form. The values of the various rate and equilibrium constants and parameters characteristic of this scheme are summarized in Table I. A simplified version of this scheme (Jain et al., 1986a–d; Jain & Berg, 1989) was used to emphasize only the binding of the enzyme from aqueous phase to the interface (E to E* step).

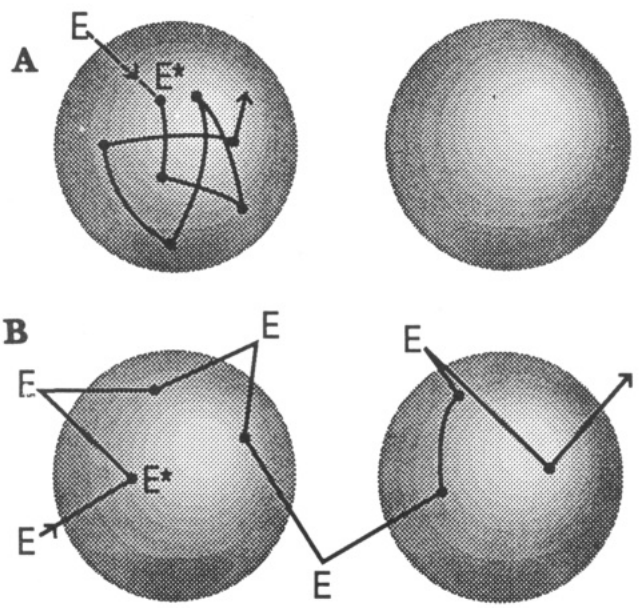

FIGURE 2: Schematic drawing to illustrate some key features of interfacial catalysis on vesicles in the scooting and the hopping modes. (A) In the scooting mode when the vesicle to enzyme ratio is >5, there is at most one enzyme per vesicle. Due to the high affinity (K_D < 0.1 pM) of PLA2 for DMPM vesicles, the bound enzyme (E*) does not leave the vesicle even when all of the substrate in the outer monolayer of the target vesicles is hydrolyzed. Therefore, excess vesicles are not hydrolyzed by the enzyme added initially unless the vesicles are allowed to fuse, the bound enzyme is forced to undergo intervesicle exchange, or the excess vesicles are hydrolyzed by adding excess enzyme so that there is at least one enzyme per vesicle. (B) On the other hand, during catalysis in the hopping mode, the enzyme desorbs from the vesicle surface, and thus all vesicles are ultimately hydrolyzed even if the vesicle to enzyme ratio is $\gg$1.

the catalytic turnover cycles. The kinetics of transbilayer or intervesicle exchange of the enzyme, substrate or product molecules between the ensemble of vesicles present in the reaction mixture is negligibly slow in bilayers on the time scale of the overall reaction (Cevc & Marsh, 1987; Jain, 1988); therefore such processes do not influence the kinetics of catalysis in the scooting mode.

Such considerations suggest that, within suitable constraints, the scheme shown in Figure 1 is the simplest possible rigorous kinetic representation for an enzymatic reaction involving the binding of PLA2 to the interface and the catalytic cycle within the interface. In this series of papers, we show that this scheme quantitatively accounts for the observed kinetic characteristics of interfacial catalysis by PLA2. In this paper, we interpret the progress curve for the hydrolysis of both small and large DMPM vesicles by PLA2 in the scooting mode in terms of an integrated Michaelis–Menten rate equation under the steady-state condition to obtain the rate parameters. Interpretation of the parameters in terms of the rate constants in Figure 1 requires the explicit assumption that $k_{-2} \ll k_3$, which is experimentally demonstrated in the second paper in this issue (Ghomashchi et al., 1991a). Independent methods for the determination of the interfacial binding equilibria for products (K_P), substrate analogues (K_S), calcium (K_{Ca}), and competitive inhibitors (K_I) to the active site are developed in the third paper in this issue (Jain et al., 1991a). Finally, the use of scooting mode analysis to study substrate specificity, the aggregation state of PLA2, and activation is described in the last three papers (Ghomashchi et al., 1991b; Jain et al., 1991b,c).

Experimental Procedures

All studies reported in this paper were carried out on PLA2 from pig pancreas isolated as described by Niewenhuizen et al. (1974). It may be noted that some of the commercially available preparations of PLA2 were also tried. These preparations were found to have significant amounts of impurities, and, for example, several batches of the preparation from Sigma (St. Louis) on HPLC showed two peaks with PLA2 activity. DMPM (lithium salt) was prepared from dimyristoylphosphatidic acid disodium salt (Avanti) by esterification with diazomethane and demethylation (Jain & Gelb, 1991) or by a complete synthesis as described elsewhere (Jain et al., 1986a). DTPM was prepared as described (Jain et al., 1986a). All other reagents were analytical grade. The acyl chain homogeneity of the phospholipid samples was checked by gas chromatography of the methyl esters of the released fatty acids (Microbial ID, Newark, DE). Most of the experimental protocols used in this study are published elsewhere (Jain et al., 1986a–d; Jain & Gelb, 1991); however, protocols for working with large vesicles are developed below and specific conditions are given in the figure legends.

Preparation of Vesicles. Small sonicated vesicles of DMPM with reasonably narrow size dispersity were prepared by sonication of the frozen suspension of the lipid (10 mg/mL) in water (Jain et al., 1986a; Jain & Gelb, 1991). It may be emphasized here that the size and dispersity of vesicles depended upon the thickness of the glass tube, its diameter and volume, the tuning of the sonicator, the presence of impurities and the chain inhomogeneity of the phospholipid sample, the concentration and the nature of the salt and pH of the aqueous phase, the concentration of the lipid, and the duration and temperature of storage of the vesicle preparation. Additional precautions were necessary for work at higher calcium concentrations because the kinetics of fusion of small vesicles had a second or higher order dependence on the concentration of vesicles, and the rate also depended on the presence of the multivalent ions and the degree of ionization of the surface charges. The effect of the chain length inhomogeneity should also be considered. For example, with a DMPM preparation containing 97% myristoyl chains (2.2% lauroyl and 0.8% palmitoyl), relatively stable vesicle preparations were obtained whose average diameter was about 23 nm compared to about 35 nm for the vesicles obtained from DMPM with more than

99.9% myristoyl chains. The sonicated vesicle preparations were usually stable for more than 8 h. However, changes in the size and dispersity of vesicles during the kinetic studies was avoided by eliminating protocols that lead to pH shock or to locally high concentrations of divalent ions, by minimizing the turbulence and cavitation during the mixing in the reaction vessel, by using low ionic strength (about 10 mM NaCl), and by keeping the concentration of vesicles low. Such precautions were necessary because, under certain conditions, vesicles in the reaction mixture fuse in a few seconds [see Jain et al. (1986a, 1991c) and Nir et al. (1983)].

Larger vesicles of relatively uniform size (20–100 nm) and low dispersity were prepared by extrusion of a hydrated suspension of DMPM in 20 mM NaCl solution at 40–55 °C under pressure (150–500 psi) through Nucleopore filters of standard pore size (Nayar et al., 1989). In our experience, the ultrafiltration devices made of polycarbonate, such as stirred cells from Amicon or Pharmacia, were superior to the Thermobarrel Extruder (Liposome Inc., Vancouver, BC) made of stainless steel. While the ease of temperature control in the Extruder made it a useful and convenient device, the DMPM vesicles seemed to pick up metal ions sufficient to influence their size and dispersity, although the problem was less acute in 20 mM NaCl solution. In these extruded preparations of vesicles there was a significant and irreproducible loss of lipid, and it was necessary to determine the lipid concentration in each preparation. Also as expected, compared to sonicated vesicles at the same bulk lipid concentration, in preparations of larger vesicles, the concentration of vesicles was lower and they were more stable, for several days in some cases. Larger vesicles obtained during the course of the kinetic analysis by spontaneous fusion of smaller vesicles had a broad size dispersity, and they were quite adequate for the measurement of initial rates of hydrolysis required for monitoring kinetics in the presence of inhibitors (Jain et al., 1989a, 1991a). Larger vesicles of uniform size were required for the analysis of the whole progress curve at high calcium (>0.8 mM). For most other experiments, small sonicated vesicles were adequate. For general considerations on handling, manipulation, and properties of phospholipid vesicles see Papahadjopoulos and Kimelberg (1975), Szoka and Papahadjopoulos (1980), and Jain (1988).

Kinetic Studies. Hydrolysis of DMPM vesicles by PLA2 in the scooting mode was monitored with a pH-stat (e.g., ETS822, or the TTT60, REC61, and autoburette based systems from Radiometer) equipped with a high-speed mechanical stirrer (e.g., Radiometer TTA60 or TTA80) and a water-jacketed thermostated vessel maintained at 22 °C (Jain et al., 1986a; Jain & Gelb, 1991). Nitrogen was continuously passed over the reaction solution (about 50 mL/min) to prevent absorption of carbon dioxide. A typical run consisted of a 4-mL reaction mixture containing 1 mM NaCl and an appropriate concentration of calcium equilibrated at pH 8.0. The stock solution of vesicles containing 0.5–1 mg of DMPM was added to this mixture, and the pH was adjusted again to 8.0. The lipid sample was discarded if the shift in the pH after the addition of vesicles was more than 0.7 pH units as this indicated appreciable degradation of the lipid sample. Also such a pH shock in the presence of calcium could induce fusion of vesicles. After the base-line drift had subsided (typically 1–5 min), the reaction was initiated by the addition of 0.2–50 pmol of PLA2 depending upon the size of vesicles, concentration of calcium and other fusogens, and of course, the purpose of the experiment (see figure legends). The reactions were typically monitored in the autotitration mode by using 3 mM NaOH and maintained at pH 8.0. The titration efficiency was routinely checked by titration of a known amount of myristic acid solution under appropriate conditions (Jain & Gelb, 1991). For example, compared to its titer in the aqueous phase below its critical micelle concentration, the titration efficiency of myristic acid was 0.93 in DMPM vesicles and 0.87 in the product vesicles at low or high calcium. It was necessary to keep a careful watch on the background pH drifts, both up or down. Routinely, the drifts were less than 0.1 nmol per min in the absence of the substrate. Under optimum conditions used for monitoring the reaction progress curves for the hydrolysis of large substrate vesicles, drifts were less than 0.2 nmol per min. Occasional cleaning of the reaction vessel, including the titration assembly and electrodes in a detergent such as Micro (International Products Inc., Box 118, Trenton, NJ) and equilibration of the combination electrode in saturated KCl was often sufficient for attaining low background drifts.

Besides these precautions, additional steps were necessary for monitoring the whole reaction progress curves for the hydrolysis of large vesicles at higher calcium concentrations where the reaction occurred over more than 30 min. For these measurements, a rapid mixing of the various components was necessary because locally high concentrations of calcium and vesicles can lead to fusion and a heterodisperse vesicle population or to an uneven distribution of the enzyme over the vesicle population. Thus, the distribution of one enzyme per vesicle was achieved only when the enzyme solution was added and rapidly mixed with a more than 5-fold excess of vesicles. For such reasons, a stirrer speed of more than 1000 rpm was necessary. For the reaction progress curves at high calcium and also in the presence of additives or products, it was necessary to avoid turbulence and cavitation in the reaction mixture, which promoted fusion and flocculation of vesicles especially at the higher mole fraction of the products near the end of the progress of the reaction. This was probably due to the surface characteristics of the fatty acids and lysophospholipids on air bubbles. In our experience, the TTA60 or 80 (Radiometer) stirrer with a small or medium size stirring rod and a 20-mL vessel with a 3–5-mL reaction mixture was the only satisfactory titration unit. Magnetically stirred cells were not satisfactory. With all such precaution, it was possible to obtain whole reaction progress curves for the hydrolysis of large vesicles preequilibrated with up to 2.5 mM calcium under the conditions given in the legend to Figure 3, which virtually required the most rigorous control of the experimental conditions used in this series of papers. Such extensive precautions were not necessary to obtain the initial rates of hydrolysis. Here one takes advantage of the fact that the rate of fusion increased the rate of replinishment of substrate in the microenvironment of the enzyme at the interface, and fusion did not influence the overall rate because the bound enzyme did not leave the interface.

The ion-binding properties of vesicles of anionic phospholipids are not very well understood yet (Jain, 1988). For some measurements, low concentrations of calcium were used in the presence of EDTA buffers, where the concentration of free calcium was determined from standard calibration curves generated directly under the conditions used for the kinetic measurements with a calcium electrode (above 0.07 mM) or Arsenazo III indicator dye (below 0.07 mM) as described by Gratzer and Beaven (1977).

The extent of hydrolysis of vesicles obtained in the presence of an excess of PLA2 molecules per vesicle (typically 5 or more) was used as a direct measure of the amount of substrate

Table I: Definition and Values of the Various Equilibrium Constants, Kinetic Rate Constants, and Parameters Shown in the Scheme in Figure 1 for the Hydrolysis of DMPM Vesicles by PLA2 at pH 8.0 and 22 °C

parameter	value	definition	comment (ref)
v_0	320 s^{-1}	$k_{cat}/(K_{MS} + 1)$	
$N_S k_i$	35 s^{-1}	$k_{cat}/K_{MS}(1 + 1/K_P)$	at 0.6 mM Ca
K_S	0.025	k_{-1}/k_1	(Jain et al., 1991a)
K_{Ca}	0.28 mM for E		(Jain et al., 1991a)
	0.16 mM for E*		(Jain et al., 1991a)
K_{MS}	0.3	$k_3(k_2 + k_{-1})/k_1(k_2 + k_3)$	(Jain et al., 1991a)
k_{cat}	400 s^{-1}	$k_2/(1 + k_2/k_3)$	at saturating Ca
k_{cat}/K_{MS}		$k_1k_2/(k_{-1} + k_2) = k_1$	(Ghomashchi et al., 1991a)
k_1	1350 s^{-1} per mole fraction		at 0.6 mM Ca
k_{-1}	30–35 s^{-1}		at 0.6 mM Ca
		$\ll k_2$	(Ghomashchi et al., 1991a)
k_2	400 s^{-1}		if $k_3 \gg k_2$
	>400 s^{-1}		if $k_3 \ll k_2$
k_{-2}	$\ll k_3$		(Ghomashchi et al., 1991a)
K_P	0.025	k_{-3}/k_3	(Jain et al., 1991a)
k_3	>400 s^{-1}		if $k_3 \gg k_2$
	400 s^{-1}		if $k_3 \ll k_2$
k_b	4 s^{-1}		(Jain et al., 1988)
k_d	<0.00002 s^{-1}		(Jain et al., 1988)
K_D	<0.1 pM	for E* to E	(Jain et al., 1986a, 1988)

accessible to the enzyme. In all the vesicle preparations, at least 50% of the total substrate was accessible for hydrolysis, which showed that all the vesicles were unilamellar and only the substrate in the outer monolayer of the vesicle was available to the bound enzyme. Also as expected, with small sonicated vesicles (cf. Figure 4), the fraction of the total accessible substrate approached 70%, depending on their radii of curvature. Such controls were useful to ascertain whether vesicles had fused or flocculated under the experimental conditions; if so, the extent of hydrolysis per enzyme and the fraction of the total substrate accessible for hydrolysis would drop considerably.

Results

Principles and Experimental Constraints. A complete theoretical analysis of the various kinetic consequences and predictions of the scheme shown in Figure 1 as applied to interfacial catalysis in the scooting mode is developed in the Appendix to this paper. Relevant equations are given in the text at appropriate points. In this treatment the rate and equilibrium parameters are defined as for the standard treatment of enzyme kinetics (Fersht, 1985; Jencks, 1969; Segel, 1975), and significant differences are elaborated in the appropriate context. All definitions and quantitative relationships (given in the text as equations with prefix A) used in these papers also refer to those given in the Appendix and are summarized in Table I. The implicit and explicit assumptions used to derive the relationships between the various interfacial kinetic and equilibrium constants are also given in the Appendix in a suitable context, and the experimental basis for these is developed in this and the accompanying papers, where we have included appropriate equations in the text. The Appendix is self-contained, and for a full appreciation of the experiments that explore the whole Michaelis–Menten space for interfacial catalysis in the scooting mode, the reader is encouraged to become familiar with the notations, definitions, conventions, and formalisms, as well as the underlying assumptions for the overall treatment. We also believe that this treatment is general, and it should be of value for the interpretation of biological interfacial catalysis on suitable matrices.

The overall strategy for using the analysis in the Appendix to obtain the rate and equilibrium parameters was based on the following considerations, conditional variables, and constraints: (a) The binding of PLA2 to DMPM vesicles was of high affinity; therefore, the E to E* step was not a part of the catalytic turnover in the steady state. Under this condition, the initial rates did not depend on the bulk concentration of vesicles. (b) When all of the enzyme is bound to the vesicle, the concentration of substrate that E* "sees" is not the bulk concentration, but it is best expressed as the probability of finding a substrate in a given surface area for the formation of E*S. This is best expressed in mole fraction units. (c) In the next paper, Ghomashchi et al. (1991a) show that the catalytic step is essentially irreversible and that the E*S complex partitions mainly toward the reaction products, i.e., $k_3 \gg k_{-2}$ and $k_2/k_{-1} > 10$. (d) The value of the interfacial Michaelis constant of $K_{MS} = 0.3$ mol fraction was obtained by independent methods (Jain et al., 1991a). (e) A protocol based on the protection of the catalytic site was also developed (Jain et al., 1991a) for obtaining values of the interfacial equilibrium dissociation constants for products (K_P) and inhibitors (K_I) bound to E*. (f) The rates of intervesicle exchange and transbilayer movement of the substrate or product molecules were assumed to be negligible, as were the differences in the surface areas of substrate, products, and additives such as inhibitors. (g) Other experimental boundary conditions that are necessary for the interpretation of the integrated reaction progress curve were that there was at most one enzyme per vesicle; fusion of vesicles did not occur during the course of hydrolysis; and dispersity of vesicles could be reasonably controlled so that it did not influence the overall shape of the reaction progress curve. The validity of these experimental boundary conditions and constraints has been established with reasonable certainty in earlier papers (Jain et al., 1986a–d; Jain & Berg, 1989) and further substantiated in this series of papers in the appropriate contexts. Finally, it may be emphasized that such constraints limit only the contribution of the parallel kinetic processes without compromising the underlying catalytic mechanism.

The Progress Curve. A typical reaction progress curve for the hydrolysis of large DMPM vesicles by PLA2 is shown in Figure 3. In this experiment, the vesicle to enzyme ratio was kept above 5. According to the Poisson distribution for the random binding of enzymes to vesicles, a vesicle to enzyme ratio greater than 5 insures that the probability of having more than one enzyme per vesicle is less than 2%. Also as discussed in the Appendix (eqs 30–37), a more complex progress curve develops if there is more than one enzyme molecule per vesicle. This is because the observed progress curve will be a superposition of individual reaction progress curves for each of the

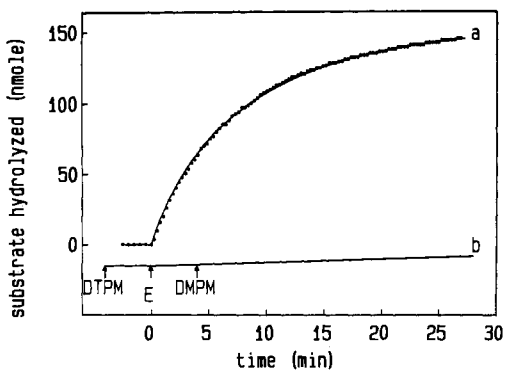

FIGURE 3: Reaction progress curve (curve a) for the hydrolysis of large extruded DMPM (chain purity >99.9%) vesicles equilibrated with 0.6 mM calcium and 1 mM NaCl at 23 °C, pH 8.0. The reaction was initiated with 1.5 pmol of (0.02 μg) pig pancreatic PLA2. For curve a, total DMPM = 1.6 μmol in 4 mL of reaction mixture; the fraction of the total substrate hydrolyzed at the end of the reaction progress curve = 0.09, and the fraction of the available substrate hydrolyzed = 0.18. The theoretical fit (smooth line) to eq A12 gave N_S = 94400, v_0 = 320 s^{-1}, and k_i = 0.085 min^{-1}. The value of the chi square = 0.09, and the deviation in the residuals along the x axis between the theoretical and experimental data points was less than 1%. (Bottom, curve b) Vesicles of DTPM (0.2 mg) were preequilibrated at 2.5 mM calcium with 10 pmol of PLA2. After 4 min, 0.7 mg of DMPM preequilibrated at 2.5 mM calcium was added to initiate the reaction. A lack of hydrolysis showed that PLA2 bound to DTPM did not exchange. The hydrolysis began immediately after mixing if the vesicles were able to fuse, as would be the case if the two vesicle populations were not preequilibrated at higher calcium concentration.

populations of vesicles containing 1, 2, 3, or more bound enzymes per vesicle. Such a system is not as readily interpreted to obtain the kinetic parameters.

The shape of the progress curve shown in Figure 3 was similar to that for most simple enzyme–substrate systems that obey Michaelis–Menten kinetics. A unique feature of the scooting model system was that the fraction of the total substrate hydrolyzed changed with the size of the vesicles and the amount of the enzyme, even though the equilibrium for the reaction lies close to 100% in favor of the products. The amount of substrate hydrolyzed at the end of the reaction, i.e., the extent of hydrolysis, increased linearly with the amount of enzyme as long as the vesicle to enzyme ratio was kept larger than 5. The linearity between the extent of hydrolysis and the amount of added enzyme was a direct consequence of the fact that the enzyme does not hop from vesicle to vesicle (Figure 2) so that only a fraction of the total substrate, accessible to the bound enzyme, was hydrolyzed. As also shown in Figure 3 (curve a), the progress curve was completely described by equation A12 for the case where there is no inhibitor, i.e., X_I = 0:

$$k_i t = -\ln [1 - P_t/P_{max}] + (k_i N_S/v_0 - 1)P_t/P_{max} \quad (A12)$$

Equation A12 is the integrated Michaelis–Menten rate equation for the scheme in Figure 1 under the steady-state approximation and with the concentration of enzyme in the aqueous phase (E) equal to zero during the entire reaction progress. It contains both a zero-order term (linear in P_t/P_{max}) that contributes mostly at early times and a first-order term (logarithmic in P_t/P_{max}) that dominates toward the end of the reaction. From such a curve, three parameters were obtained. The number of substrate molecules in the outer monolayer of the target vesicle, N_S, was obtained from the extent of hydrolysis:

$$P_{max} = C_E N_S \quad (A11b)$$

The initial velocity per enzyme molecule, v_0, and the first-order relaxation constant, k_i, were obtained by curve-fitting the reaction progress curve by the nonlinear regression method. The significance of these two rate parameters is defined by the following rearranged equations from the Appendix with X_I = 0:

$$v_0 = k_{cat}/K_{mS}(1 + 1/K_{mS}) \quad (A7)$$

$$N_S k_i = k_{cat}/K_{mS}(1 + 1/K_P) \quad (A10)$$

Equation A7 is the standard Michaelis–Menten equation, which relates the initial velocity per enzyme molecule, v_0, to the concentration of substrate in the interface expressed as its mole fraction. In the absence of additives (i.e., X_I = 0), the mole fraction of substrate in the bilayer is initially equal to 1. As defined here, v_0 is the turnover number at the maximal substrate concentration, i.e., the mole fraction of substrate = 1. It differs from the standard turnover number, which is the initial velocity per enzyme molecule under saturating conditions when the concentration of the free enzyme is zero. $N_S k_i$ is the apparent second-order rate constant, i.e., the effective k_{cat}/K_{MS} value, which includes product inhibition, for the lipolysis reaction in vesicles. This parameter is independent of the size, N_S, of the vesicles as k_{cat} and K_{MS} are the fundamental kinetic parameters for the activity of the enzyme in the interface.

Effect of the Size of Vesicles. If intervesicle exchange of enzyme and lipids is negligible, the kinetics of hydrolysis of an ensemble of vesicles can be monitored under the conditions where there is at most one enzyme per vesicle. Under these conditions, N_S was readily obtained as the ratio of the total moles of substrate hydrolyzed at the end of the reaction divided by the moles of the enzyme in the reaction mixture (cf. eq A11b). Thus the extent of hydrolysis increased with the amount of enzyme in the reaction mixture; however, N_S remained constant because it is the number of substrate molecules in the outer monolayer of the target vesicle (cf. eq A8). As expected, the value of N_S changed with the size of the vesicles, which can be altered by inducing fusion of smaller vesicles or by using appropriate procedures for the dispersion or extrusion of DMPM. For vesicles used in generating the reaction progress curve in Figure 3, the value of N_S was 94000, and in other studies reported in this paper N_S values ranged from 3200 to 110000. For example, extrusion of DMPM dispersions through filters of 30–100-nm diameter (filled circles in Figure 4, curve a) provided vesicles of the corresponding size. Here the square root of N_S increased linearly with the pore size of the filter through which the vesicles were extruded. Figure 4 was also used for calibrating the average size of vesicles obtained by sonication or fusion. For example, the smallest sonicated vesicles had an N_S value of 3000; however, they were quite unstable and fused appreciably in 2 h. More stable preparations of sonicated small vesicles with N_S = 4400 were routinely obtained with DMPM having a chain purity of 97% (open square in Figure 4), whereas stable vesicles with N_S = 11700 were obtained from DMPM with a chain purity of >99.9% (open circle in Figure 4). Additional evidence for the size of the small sonicated vesicles with N_S = 4400 and a diameter of 23 nm was described elsewhere (Jain et al., 1991b).

The rate of fusion of small sonicated vesicles was significant above 0.8 mM calcium (Jain et al., 1986a), and the value of N_S necessarily increased when the vesicles fused. As summarized in Figure 5 (open circles), the value of N_S increased in the presence of calcium at constant bulk concentration of DMPM. Thus, for small vesicles, over the course of the reaction progress curve fusion became significant when the

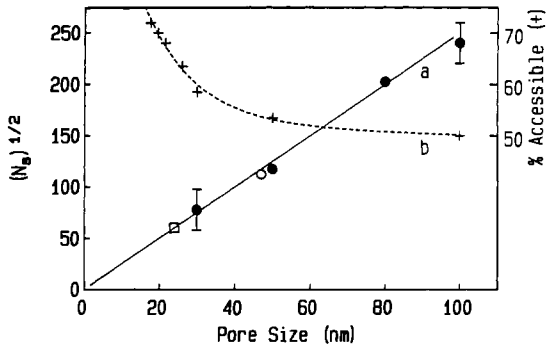

FIGURE 4: (Curve a, full line) Square root of N_S versus the pore size of the polycarbonate (Nucleopore) filters used for extrusion of the vesicles (filled circles). Other preparations (open symbols) shown here were the vesicles used for calibration of size (see text for details). (Curve b, dashed line) Fraction of the total substrate accessible for hydrolysis by excess PLA2 as a function of the size of the vesicles expressed directly in terms of the pore size or calibrated on the basis of their N_S value.

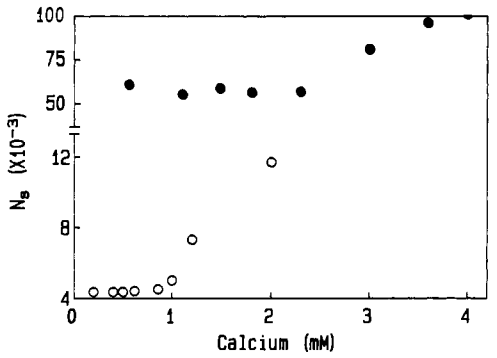

FIGURE 5: Dependence of N_S (extent of hydrolysis per enzyme) on the calcium concentration for small sonicated vesicles (open circles) and for the larger (100-nm) extruded vesicles (closed circles).

calcium concentration exceeded about 0.8 mM, whereas larger extruded vesicles of 100-nm diameter (closed circles in Figure 5) were stable, as monitored by the extent of hydrolysis, as long as the calcium concentration remained 2.5 mM or less. Since N_S values were obtained from the extent of hydrolysis from a progress curve with the one-enzyme–one-vesicle situation, it was an integrated measure of the average size of the fused vesicles. These results showed that the size of the vesicles could be maintained constant within a reasonable range of the concentration of calcium and bulk concentration of DMPM, and they served as useful controls to obtain the window of conditions used in the experiments described below, where the effects of calcium on the kinetic parameters have been dissected from the effects of calcium on the size of vesicles. Fortunately, for most studies involving characterization of the whole reaction progress curve, the calcium concentrations above 1 mM were not usually required.

Not only did the fraction of the total substrate accessible to the enzyme remain constant during the course of hydrolysis but the integrity of vesicles was also maintained even when most of the surface of vesicles was covered by PLA2. As shown in Figure 6, the fluorescent dye, calcein was released only very slowly on the addition of PLA2 or even after all the substrate in the outer monolayer had been hydrolyzed. A slow leakage in the PLA2-containing vesicles was probably due to the formation of the products. The vesicle contents would have leaked out immediately if the binding of PLA2 or the formation of the products induced a nonbilayer phase. The ratio of phospholipid molecules in the two monolayer halves of a bilayer also changed with the radius of curvature of vesicles.

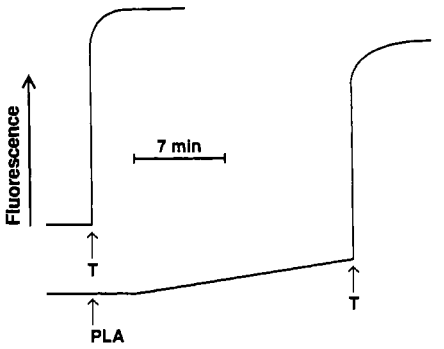

FIGURE 6: Time course of release of calcein trapped in 1-palmitoyl-2-oleoyl-*sn*-glycero-3-phosphoglycerol vesicles after binding and hydrolysis by PLA2. (Top) Triton X-100 (2 mM) added at $t = 0$; (bottom) 1 μg of PLA2 added at $t = 0$, and then Triton X-100 (2 mM) added at $t = 20$ min.

As shown in Figure 4 (curve b, dotted line), the fraction of total substrate hydrolyzed in the presence of an excess of PLA2 (more than five enzyme molecules per vesicle) changed from 71% to 50% as the size of the unilamellar vesicles increased. On the other hand, as expected, only 5–8% of the total substrate was hydrolyzed in multilamellar vesicles (data not shown). This protocol provided a convenient method to measure the accessible substrate on vesicles. These studies also demonstrated that the rate of transbilayer movement of the substrate or product molecules was very slow, with half-times greater than 3 h under the conditions of at most one enzyme per vesicle. From these and related results [e.g., see Jain et al. (1986a–d, 1991a)], it was concluded that PLA2 did not promote transbilayer movement of the substrate or the products over a <30-min period, that it did not cause a disruption of the bilayer organization, and that it did not solubilize the substrate during the course of the catalytic turnover. Although these studies were carried out with PLA2 from pig pancreas, in key experiments similar results were obtained with PLA2s from other sources, including venoms (Jain et al., 1991b).

The interpretation of N_S was based on the assumption that during the course of hydrolysis the enzyme remained bound to the target vesicle so that it did not exchange with excess vesicles. Not only was this assumption consistent with the observation that N_S changes with the size of vesicles, but by several techniques it has been shown that the E to E* equilibrium was completely in favor of E* on small as well as large DMPM or DTPM vesicles [e.g., see Jain et al. (1986a–d)]. The essentially irreversible binding of PLA2 to DMPM vesicles was most convincingly demonstrated by the experiment shown in Figure 3 (curve b). Here PLA2 bound to large vesicles of the nonhydrolyzable substrate analogue DTPM did not exchange with DMPM vesicles. In this experiment, addition of PLA2 to vesicles of DTPM followed by addition of DMPM vesicles did not result in the formation of product because the enzyme bound to DTPM vesicles was not able to hop to the DMPM vesicles.

The studies summarized in Figures 3–6 showed that the enzyme bound to the bilayer interface did not exchange readily with excess vesicles. This held true not only for small and large vesicles of DTPM and DMPM but also for vesicles containing the products of hydrolysis or up to 20% of a number of amphiphilic additives including other phospholipids [e.g., see Jain et al. (1991a,c) and Ghomashchi et al. (1991b)]. It is also important to note that in all such situations the enzyme bound to the interface remained fully catalytically active even after the formation of products ceased. This was demonstrated by the fact that at the end of the reaction progress curve the

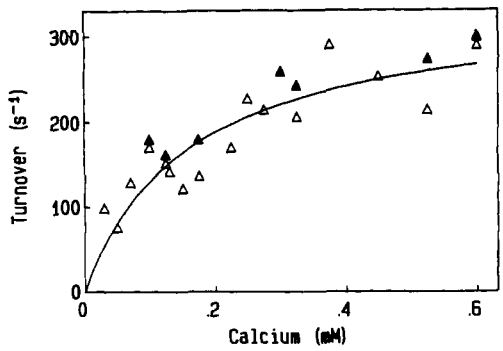

FIGURE 7: Dependence of (open triangles) $N_S k_i$ (× 7.5) and (closed triangles) v_0 on the free calcium concentration. DMPM (0.43 mM) vesicles of different sizes (not distinguished here) were used for these studies. The rate parameters v_0 and $N_S k_i$ were obtained by curve fitting the whole reaction progress curves as shown in Figure 3. The theoretical curve for v_0 shown here was fitted with the assumptions given under Discussion for the calcium dependence of k_{cat} with K_{MCa} = 0.17 mM. The maximum value of v_0 = 320 s^{-1} was obtained at a saturating concentration of calcium.

hydrolysis ensued if the substrate was replenished by calcium-promoted fusion of the enzyme-containing vesicles with nonhydrolyzed vesicles. Furthermore, after the reaction ceased, high salt concentrations initiated the reaction again since this caused the enzyme to hop to other vesicles [cf. Jain et al. (1986b)].

As expected, the shape of the progress curve was also influenced by the dispersity in the size of vesicles in a preparation. This problem could also be addressed quantitatively. As predicted by eqs 27–29, the main effect of increased dispersity (as in stored or in frozen-and-thawed DMPM vesicles) was to slow down the reaction as it approached the end of the hydrolysis (results not shown). This had significant effect on the fitting parameters. Indeed, the analysis given in the Appendix predicts that a noticeable change in the shape of the reaction progress curve would be observed only if the dispersity exceeded 0.2 (or 20%) in the radius, i.e., if a significant fraction of vesicles differ from the average size (N_S) by more than 45% or so. This does not appear to be a problem with the smallest sonicated or with the extruded vesicles (Nayar et al., 1989). The results described so far are consistent with the conclusion that N_S was the total number of substrate molecules present initially in the outer monolayer of the target vesicles, and the controls also served as a reminder that the consideration of the size and dispersity of vesicles was important in order to quantitatively interpret the integrated reaction progress curve. Fortunately, for studies using the initial rate of hydrolysis or others not involving a consideration of the value of N_S, such a rigorous control on the size was not necessary (Jain et al., 1989a, 1991a,c; Ghomashchi et al., 1991a,b).

The Rate of Catalytic Turnover in the Interface. Calcium is a cofactor required for the catalytic activity of PLA2 (Verheij et al., 1980, 1981; Donne-op den Kelder et al., 1983; Fleer et al., 1981; Pattus et al., 1979; Pieterson et al., 1974a,b; Slotboom et al., 1978; van den Bergh et al., 1989). The values of the interfacial catalytic rate parameters v_0 and $N_S k_i$ as a function of calcium concentration are shown in Figure 7, and the data points could be fitted to a single hyperbola with K_{Ca} = 0.17 mM and the maximum values of v_0 = 320 s^{-1} and $N_S k_i$ = 43 s^{-1}. Individual data points in Figure 7 were obtained by fitting the entire reaction progress curve to the integrated Michaelis–Menten eq A12. Here the concentration of calcium was kept below 0.6 mM, because as shown in Figure 5 the rate of fusion of vesicles became appreciable above 1 mM calcium. It is also pertinent to note that the same value of the initial rate, 320 s^{-1}, was obtained for several minutes under conditions where the vesicles were allowed to fuse during the course of hydrolysis and the rate of replenishment of the substrate was rapid. These conditions were best accomplished by adding enzyme to small sonicated vesicles soon after they are induced to fuse by calcium (Jain et al., 1986a) or by other fusogens like magnesium and polymyxin B (Jain et al., 1991c).

Discussion

In this and in the accompanying papers, the kinetics of the hydrolysis of DMPM vesicles by PLA2 in the scooting mode was explored in detail and quantitatively interpreted in terms of the scheme in Figure 1. We also established the experimental boundary conditions and the constraints of molecular organization and dynamics that allowed kinetic characterization of interfacial catalysis in the scooting mode according to Figure 1. The theoretical analysis developed in the Appendix provided a guide for elaboration of the scheme in Figure 1 and for the design of the experiments described in this series of papers that served as a basis for obtaining the values of the kinetic rate constants and parameters. The broader implications of these studies arise from the fact that virtually the whole Michaelis–Menten kinetic space has been explored, including the effects of the concentration of the substrate, products, enzyme, activators, calcium, and competitive inhibitors with the set of kinetic and equilibrium parameters summarized in Table I. The direct significance of results reported in this paper is discussed below at three levels: (a) specific activity of PLA2 at the interface of DMPM vesicles; (b) the values of the kinetic rate constants for catalytic turnover in the interface as summarized in Table I; and (c) the role of calcium in the catalytic turnover.

Specific Activity of PLA2. Measurement of true initial rates of interfacial catalysis in the scooting mode has certain advantages over other assay protocols. Since K_D for E* is small, the rate of hydrolysis is not sensitive to the bulk concentration of the lipid, the presence of lipophilic additives (Jain et al., 1989a,b; 1991a), and the gel–fluid phase properties (Jain et al., 1988). With this system, it was possible to obtain the values of the interfacial equilibrium constants (Jain et al., 1991a), to establish the presence of impurities in a PLA2 preparation (Jain et al., 1988, 1991b), and to unequivocally ascertain substrate specificity (Ghomashchi et al., 1991b), competitive inhibition (Jain et al., 1989a, 1991), and the effect of activators (Jain et al., 1991c) without any complications from the E to E* step or other nonspecific effects (Jain & Jahagirdar, 1985b; Jain & Berg, 1989; Jain et al., 1989b). Moreover, not only did DMPM serve as a substrate for PLA2s from many different sources, but it was possible to obtain the number of catalytically functional PLA2 molecules in a preparation from the extent of hydrolysis measurements (Jain et al., 1991b). In short, by monitoring interfacial catalysis in the scooting mode, one can virtually eliminate the effects often associated with the "quality of interface" under a wide range of experimental conditions and thus explicitly characterize the effects on the catalytic steps.

PLA2 is highly active on DMPM vesicles without any additives. In Table II the initial rate per enzyme (v_0) is compared with that on other interfaces, including detergent-dispersed mixed micelles. The v_0 = 320 s^{-1} corresponds to 1350 μmol per minute per milligram of PLA2 (units) at 23 °C and about 3300 units at 40 °C. These values compared favorably with specific activities of about 900 units reported for anionic phospholipids and about 100–300 units for zwitterionic phospholipids alone or codispersed in deoxycholate at optimal mole ratios at 23 °C (de Haas et al., 1971, 1990; Bonsen et

Table II: Specific Activities for Pig Pancreatic PLA2 at Different Interfaces at 22 °C

substrate	initial rate (μmol/min·mg of PLA2)[a]	interface/conditions (ref)
DMPM	1350	bilayer vesicles; no additives
	3340	at 40 °C; as above
	900	mixed micelles with DOC (1:1)
DMPG	900	mixed micelles with DOC (1:1)
DMPC	280	in the presence of products (1)
	110	mixed micelles in DOC (1:1) (2)
	<10	mixed micelles in Triton X-100
dioctanoyl-GPC	1200	no additive (3)
dioctanoyl-GPM	4120	no additive (3)

[a] Data from (1) Jain and Jahagirdar (1985a), (2) de Haas et al. (1990), and (3) Jain and Rogers (1989). All other numbers are from this study. Abbreviations: DOC, deoxycholate; GPC, *sn*-glycero-3-phosphocholine; GPM, *sn*-glycero-3-phosphomethanol.

al., 1972; Apitz-Castro et al., 1982; Jain et al., 1982; Jain & Jahagirdar, 1985a; von Oort et al., 1985a,b; Jain & Rogers, 1989; de Haas et al., 1990). Such comparisons demonstrated that the catalytic efficiency of PLA2 on DMPM vesicles in the absence of additives was at least as good as, if not better than, that observed on substrates comicellized with optimal mole fractions of detergent. The 30% lower activity on detergent-dispersed micelles can also be explained in the following way. Results summarized in Table II were obtained under comparable conditions where all the enzyme was bound to the interface, and the rate of hydrolysis by bound PLA2 would be determined by the steps in the catalytic cycle. As predicted by eq A7, lower v_0 values are expected in mixed micelles resulting from surface dilution by the detergent. For example, a specific activity of 900 units for dimyristoylglycero-*sn*-3-phosphoglycerol at mole fraction 0.5 (de Haas et al., 1990) would correspond to a specific activity of 1200 units at mole fraction 1 if $K_{MS} = 0.3$ in mole fraction units. These effects related to dilution of the substrate at the interface are considered further (Jain et al., 1991a).

At this stage, it appears reasonable to briefly consider other factors that could influence specific activities:

(a) The effects associated with a shift in the E to E* step are spread over a 10^{10}-fold range as values of K_D for E* can vary from <10 pM on anionic DMPM vesicles to >1 mM on zwitterionic PC vesicles (Jain et al., 1986b). As reviewed elsewhere (Jain & Berg, 1989), they account for several anomalous effects associated with the change in the thermotropic and solute-induced isothermal phase properties of the interface.

(b) The effects related to true substrate specificity can also be now dissected (Jain & Rogers, 1989; Ghomashchi et al., 1991b), and these effects appear to fall in a considerably smaller range, and only in some extreme cases were the rates of hydrolysis of different substrates different by more than a factor of 10.

(c) Mixed micelles with a different detergent (e.g., deoxycholate vs Triton X-100 in Table II) or with an increase in the detergent concentration could have considerably larger effects because under such conditions the molecular organization, dynamics, and polymorphism of mixed micelles changes, which could influence the rate of replenishment of the substrate that the enzyme "sees" on the micelle during the course of hydrolysis. As discussed in the Appendix, this arises from a fundamental corollary of the steady-state condition, i.e., the local environment of the enzyme must not change during the time course of the measurement. For the values of initial enzymatic velocities in mixed micelles to be free of rate terms involving micelle dynamics, the substrate replenishment rate must be fast, on the 10–100 ms time scale (see Appendix). Thus it is likely that the v_0 measured in mixed micelles changes in response to the mixed micelle concentration and composition because these dynamic processes are largely collisional and slow (Nichols, 1988; Nichols & Ozarowska, 1990). We estimate that these effects due to substrate-limited rates in micelles could cause well over a 100-fold change in the observed rates.

(d) One must consider a whole range of effects associated with changes in the intrinsic molecular surface areas, organization, lateral distribution and miscibility of the substrate, products, and additives. As shown elsewhere (Ghomashchi et al., 1991b; Jain et al., 1986a,c, 1988), such effects related to the surface density of the substrate under extreme conditions would probably change the rate of overall catalytic turnover by less than a factor of three.

The Kinetic Rate Constants. The relationships developed in the Appendix to describe the scheme in Figure 1 are symmetrical and simple in form, and therefore are easily applied. Furthermore, as described below, they provided ample opportunity for a cross check on the values of the various parameters and also provided a rigorous basis for obtaining the rate and equilibrium parameters summarized in Table I. Within the constraints outlined above, the reaction progress curve was fitted to eq A12 to obtain values of two parameters related to interfacial catalytic turnover, $N_S k_i$ and v_0, which are related to the Michaelis–Menten parameters K_{MS}, K_P, and k_{cat} by

$$v_0 = k_{cat}/(1 + K_{MS}) \quad \text{(A7)}$$

$$N_S k_i = k_{cat}/[K_{MS}(1 + 1/K_P)] \quad \text{(A10)}$$

From eq A7 with $v_0 = 270\ s^{-1}$ at 0.6 mM calcium (Figure 7) or $320\ s^{-1}$ at saturating calcium (see below), $k_{cat} = 400\ s^{-1}$ at infinite substrate mole fraction, with the value for $K_{MS} = 0.3$ as determined in Jain et al. (1991b). The value of K_P was measured (Jain et al., 1991a) as 0.025 in mole fraction units. From the values of $K_{MS} = 0.3$ and $K_P = 0.025$, the $N_S k_i/v_0$ ratio is calculated to be 0.11 according to

$$N_S k_i/v_0 = (1 + 1/K_{MS})/(1 + 1/K_P) \quad \text{(A15)}$$

This agrees favorably with the experimental results in Figure 7 where the ratio $N_S k_i/v_0$ is seen to have a value of about 0.13 at all calcium concentrations up to 0.6 mM. A similar value of the $N_S k_i/v_0$ ratio was also obtained from the kinetic results in the presence of competitive inhibitors with experiments based on eqs A19 and A20 and is developed in the third paper in this series (Jain et al., 1991a). The agreement in the value of this ratio obtained by three independent methods leaves little doubt about our estimation of the value of these rate parameters.

These calculations could be extended further to obtain values of some of the rate constants in the scheme in Figure 1. Oxygen-18 solvent exchange studies described in the second paper in this series (Ghomashchi et al., 1991a) gave the condition that $k_3 \gg k_{-2}$. Under this condition, eqs 2a and 2c of the Appendix can be simplified to give

$$k_{cat} = k_2/(1 + k_2/k_3) \text{ and } k_{cat}/K_{MS} = k_1 k_2/(k_{-1} + k_2)$$

Heavy-atom isotope effect studies described in the second paper in this series (Ghomashchi et al., 1991a) gave the condition that $k_2 \gg k_{-1}$, which yields

$$k_{cat}/K_{MS} = k_1 = 1350\ s^{-1}\ (\text{mole fraction})^{-1}$$

The rate of dissociation of the substrate from E*S, k_{-1}, can also be estimated in the following way. The substrate disso-

ciation constant (K_S) is expected to be similar to the dissociation constant for the nonhydrolyzable substrate analogues *sn*-3-DTPM, *sn*-1-DMPM, and *sn*-3-DMPM, determined to be 0.02–0.03 mole fraction (Jain et al., 1991a). Thus the value of $k_{-1} = 35\ s^{-1}$ was estimated by using $k_1 = 1350\ s^{-1}$, which satisfies the condition from the heavy-atom isotope effect experiments, i.e., $k_2 \gg k_{-1}$.

At this point, values for many of the interfacial rate constants have been estimated as listed in Table I. However, the individual values for the rate constants k_2 and k_3 cannot be determined from the present data. Since

$$k_{cat} = k_2/(1 + k_2/k_3)$$

both k_2 and k_3 must be greater than k_{cat}. If the chemical step was slow compared to the release of products from E*P, then $k_{cat} = k_2 = 400\ s^{-1}$. On the other hand, if the release of products was the rate-limiting step for the breakdown of E*S, then $k_{cat} = k_3 = 400\ s^{-1}$. From the present results, it was not possible to determine which of these extremes, if any, was relevant for interfacial catalysis by PLA2. The resolution of this point will require the kinetic analysis of a set of substrates that are expected to have greatly different k_2 values but very similar k_3 values, for example, by substitution of the *sn*-2 ester with a different element such as sulfur. It is, however, interesting to note that values of $k_3 = 400\ s^{-1}$ and $K_P = 0.025$ would give a value of $k_{-3} = 16\,000\ s^{-1}$, which may be close to the rate constant for a process limited by two-dimensional diffusion of the components in the interface (Jain & Berg, 1989).

Role of Calcium in Catalysis. The effects of changing the calcium concentration on v_0 and $N_S k_i$ are summarized in Figure 7. The apparent K_{MCa} for both of these parameters was 0.17 mM and the maximum value of v_0 was $320\ s^{-1}$. This kinetically determined value of K_{MCa} is in agreement with the value of the dissociation constant $K_{Ca} = 0.16$ for the enzyme at the interface (Jain et al., 1991a; Slotboom et al., 1978). This agreement between K_{MCa} and K_{Ca} suggests that the effect of calcium on the rate parameters is due to its binding to the catalytic site on E* rather than on interaction of the metal ion with the interface. The K_{Ca} for the enzyme in the aqueous phase is not significantly different (Jain et al., 1991a), which suggests that calcium is not required for the binding of the enzyme to DMPM vesicles (Jain et al., 1986b). The correspondence between the K_{Ca} values obtained between the kinetic and equilibrium binding measurements is significant because in earlier studies using micellar substrates an apparent dissociation constant of about 2 mM was reported (Verheij et al., 1981). The origin of this discrepancy is not established yet, and the influence of calcium on the individual rate constants involved in the catalytic cycle remains to be elucidated.

To recapitulate, the kinetics of interfacial catalysis in the scooting mode has provided a method to obtain the interfacial catalytic parameters summarized in Table I. Although kinetic results do not necessarily constitute a proof, the consistency of the results covering virtually the whole Michaelis–Menten space involving effects of calcium, substrate, product, competitive inhibitors (Jain et al., 1991a), and apparent activators (Jain et al., 1991c) over the whole concentration range is unprecedented for interfacial catalysis, and it is gratifying. These studies bring the kinetic analysis of interfacial catalysis by PLA2 to the same level of detail with which water-soluble enzymes have been explored.

Acknowledgments

M.K.J. expresses appreciation for the inspiration by (late) Professor Peter Lauger (Konstanz): "If these constants are there, there must be a way to get to them." We thank Professor Michael Gelb for very stimulating discussions, useful comments, editorial help on numerous drafts of the manuscripts, and for delaying the publication of his results described in the next paper in this issue.

Appendix: Interfacial Catalysis in the Scooting Mode

(1) Introduction

Enzymes acting on aggregates or surfaces sometimes display complex kinetic behavior that is difficult to interpret quantitatively. Often this is due to the difficulty of resolving the various competing processes that can occur, such as the exchange of lipids or enzymes between the ensemble of particles, and fusion and fission of such particles. Thus it is necessary to design experiments such that the influence of competing reactions or exchange processes are minimized. Within the constraints of these conditions, which require a stable surface of substrate to which the enzyme is bound, it becomes possible to study in detail the reactions taking place at the catalytic site of the enzyme without compromising the underlying catalytic mechanism. The catalytic steps in the scheme in Figure 1 are analytically elaborated in this appendix to rigorously account for the kinetics of interfacial catalysis as developed in this series of papers.

The aggregated form of the substrate necessarily brings additional considerations into the kinetic equations describing the catalytic reaction of enzymes that act on interfaces. Our approach for analyzing the features of interfacial catalysis of PLA2 in vesicles is to adapt the standard treatment of enzyme kinetics (Segel, 1975; Fersht, 1985) as it is applied to numerous cases of water-soluble substrates. *This formalism requires a perfect mixing of all reactants, at least on a gross scale, so that every enzyme on the average "sees" the same environment of substrate and product at any particular time.* In the study of enzyme kinetics on vesicles or micelles, special care has to be taken to ensure that this requirement is fulfilled.

Thus to study and interpret interfacial catalysis in the steady-state, three problems must be solved: (a) Since catalysis occurs in the interface, the fraction of the enzyme in the interface must be established. (b) The contribution from competing exchange processes must be eliminated or at least explicitly accounted for, so as to consider only the steps shown in the scheme in Figure 1. (c) An appropriate mixing of the components must be maintained so as to assure uniformity of the environment that enzyme molecules "see" during the course of hydrolysis. These problems are interrelated and depend on the size of the aggregates (vesicles or micelles) as well as on the time scales for molecular exchange between aggregates. Below we shall provide the conceptual and mathematical basis for the interpretation of the experimental data on interfacial catalysis.

(2) Kinetics on Vesicles and Micelles.

It is important to realize that each vesicle or micelle should be considered as a closed or semiclosed system with a finite number of molecules involved. This is in contrast to the water-soluble case and is the source of the mixing and exchange problems. These become particularly acute for the smallest systems, like small vesicles and micelles.

To ensure that all enzymes "see" the same environment at any particular time, it is important that all enzymes are bound at the interface; this may require sufficiently large concentrations of vesicles or micelles. Otherwise, one must know the fraction of the bound enzyme and ascertain that the progress of the catalytic reaction does not change the binding equi-

librium. Furthermore, there must be an even distribution of enzymes over different vesicles or micelles. Otherwise, the substrate in the vesicles with many enzymes will be depleted faster, and therefore the bound enzyme would "see" a different environment than one on vesicles with fewer enzymes. Such a variation in the distribution of enzyme on the particles is not a problem if the rate of exchange of enzyme and/or lipid between different vesicles or micelles is sufficiently fast to ensure that each enzyme "sees" a similar averaged environment. Often the problem is to ascertain whether this is the case. Alternatively, as described below, the distribution problem can be addressed, at least in the vesicle case, by choosing an appropriate enzyme-to-vesicle ratio.

(2a) Exchange in Micelles and Mixed Micelles. As an enzyme turns substrate into product in a micelle, its composition will change rapidly. If all molecules (lipid and enzyme) remain bound to the same micelle, the reaction will be over quickly when the 10–100 substrate molecules have been acted on. However, lipids can exchange between different micelles, and substrate can be replenished from micelles with no enzymes. In order to maintain the initial surface composition for an extended time, the exchange of lipid must be fast on the time scale of the catalytic reaction, i.e., the reciprocal of the enzymatic turnover number. This requires that lipid exchange must be faster than 10 ms or so, otherwise a steady state will develop where the apparent activity of the enzyme is determined primarily by the exchange rate of lipid between micelles.

Alternatively, continuity in the reaction progress could be maintained by the enzyme exchanging between different micelles. This must be fast on the time scale of the rate of change of the surface composition. In this limit an enzyme will convert only a few substrate molecules before going on to a fresh micelle, and a steady state can develop where the mole fraction of the substrate on the enzyme-containing micelles does not change, and the enzyme activity can be determined through standard initial rate measurements and interpreted with few additional assumptions. However, for an enzyme like PLA2, the catalytic rate is faster than 100 s^{-1}. This requires that enzyme exchange should be faster than about 100 ms. Such rate requirements are difficult to verify experimentally, and this fast-exchange problem for enzyme kinetics on micelles has never been properly addressed.

(2b) Exchange in Vesicles; Hopping vs Scooting. The situation is quite different in vesicles. First, these are substantially larger than micelles so that there is not the same problem of a rapid depletion of available substrate in an individual particle. Furthermore, the intervesicle exchange of naturally occurring phospholipids is usually slow on the time scale of the hydrolysis of vesicles by PLA2. This makes it possible to describe a vesicle as an individual and integral entity that is changing only due to the catalytic activity of the enzyme. Then, only the intervesicle exchange of enzyme remains as a key consideration. If the enzyme is hopping between vesicles and if this exchange is not fast enough, the enzymes would separate into different populations with different vesicle environments as they bind to vesicles that have had no enzymes previously. Thus as time goes on, each enzyme "sees" a different environment, and this introduces new components in the reaction progress that are determined by the intervesicle enzyme-exchange rate and not by the catalytic rate constants for the action of the enzyme within the interface.

Alternatively, if the exchange of enzyme is sufficiently rapid, there will be an averaging over all vesicles and no large differences in composition between different vesicles will occur during the course of the reaction. However, as in the micellar case, it would be very difficult to verify that the exchange rate is sufficiently rapid.

In contrast to the micellar case, the problem of enzyme exchange can be solved, at least in principle, simply by increasing the amount of enzyme so that a large number (larger than 10 or so) is bound to each vesicle. In this limit, the rate of intervesicle enzyme exchange will play no role, and every vesicle will be depleted of substrate at approximately the same rate. The drawback, of course, is that the overall reaction progress becomes very fast, although this may still be a useful limit, at least for larger vesicles with enzymes with low catalytic turnover.

The alternative is to consider the action of PLA2 in the scooting mode (Jain et al., 1986a–d; Jain & Berg, 1989) where the enzyme remains tightly bound to the vesicle surface. In this case, one must take into consideration the distribution of enzymes on the vesicles. Since the distribution of irreversibly bound enzymes on the vesicles is expected to follow a Poissonian distribution, if there are on the average N enzymes for each vesicle, the variation in this number will be $\approx N^{1/2}$, and for small values of N, the relative variation will be large. This small-number variation will lead to heterogeneities where individual enzymes are in different environments. This is because, at any given time, vesicles that contain a larger number of bound enzymes will contain more product and less substrate than vesicles with fewer enzymes. In this case, the overall reaction progress must be described as a statistical average over an ensemble of such systems. While such statistical averaging can be carried out in some cases (see section 3d below), it invariably leads to complications in the analysis of the data.

One way of avoiding the statistical problem of small-number variations is to work with large enzyme concentrations such that there are on the average at least 10 enzymes per vesicle. Thus this limit of a large enzyme-to-vesicle ratio can solve both the problem of a finite intervesicle enzyme-exchange rate and the problem of an uneven distribution. However, since the vesicles are of a limited size, this can lead instead to a crowding problem and/or to a reaction progress that is so fast that it becomes difficult to study experimentally.

The statistical distribution problem can be eliminated in the limit where enzymes are irreversibly bound to the vesicles and if there is at most one enzyme per vesicle. In this case with a small enzyme-to-vesicle ratio, all vesicles will be depleted of available substrate at the same rate or not at all, and individual enzymes will be in a common environment at all times in the reaction progress. Thus there are no heterogeneities between different enzymes, and the data analysis is straightforward and leads to particularly simple relationships that are analogous to those derived in standard texts on enzyme kinetics. Furthermore, as discussed in the main text, the validity of the scooting-mode conditions are easily verified experimentally.

(2c) Boundary Conditions and Mathematical Model. The minimal reaction scheme required to describe the activity of PLA2 is given in Figure 1 of the main text. It includes a step, $E \rightleftharpoons E^*$, where the enzyme binds to the surface of the aggregated substrate. The reactions in the box are the interfacial steps where substrate is dislodged from the surface and enters the catalytic site, followed by the catalytic step and product release.

In the following we shall describe the scooting-mode kinetics where an enzyme remains bound at the same vesicle throughout the reaction. Let us first consider the reaction

kinetics on one vesicle with one enzyme bound. This one-vesicle–one-enzyme case represents the elementary basis from which more complicated situations can be described.

There are two main differences in this system from the general enzyme kinetics taking place in bulk solution. First, individual vesicles are assumed to be closed systems with no exchange between them, either of enzyme, substrate, or products. Secondly, the geometric arrangements of molecules in the membrane precludes the totally free variation of substrate, product, and inhibitor concentrations that often form the basis of the study of enzyme reactions in bulk solution. Thus, inhibitor and substrate concentrations cannot easily be varied independently, nor can one of them be increased beyond the level where it totally makes up the surface.

The most natural unit to use for the surface concentrations of the reactants is the mole fraction since this will express the probability of finding a certain kind of molecule at a certain position in the surface. Thus the association rate of the substrate, both the products, or inhibitor (S, P, or I, respectively) to the catalytic site of the enzyme will be proportional to the mole fraction X_S, X_P, or X_I present in the surface. The overall reaction scheme on the vesicle can be analyzed in the same way as the usual bulk reaction simply by using the mole fraction of components instead of the bulk concentrations. At the steady state, the number of product molecules produced per enzyme per unit time can be expressed as

$$v = \frac{K_{MP}k_{cat,S}X_S - K_{MS}k_{cat,P}X_P}{(1 + X_I/K_I)K_{MS}K_{MP} + K_{MP}X_S + K_{MS}X_P} \quad (1)$$

where K_{MS}, K_{MP}, $k_{cat,S}$, and $k_{cat,P}$ are well-known combinations of the basic rate constants in the reaction scheme and can be found in standard text books [e.g., Segel (1975)]. For a three-step reaction like the scheme in Figure 1, they can most conveniently be expressed as

$$1/k_{cat,S} = 1/k_2 + (1/k_3)(1 + k_{-2}/k_2) \quad (2a)$$

$$1/k_{cat,P} = 1/k_{-2} + (1/k_{-1})(1 + k_2/k_{-2}) \quad (2b)$$

$$K_{MS}/k_{cat,S} = (1/k_1)[1 + (k_{-1}/k_2)(1 + k_{-2}/k_3)] \quad (2c)$$

$$K_{MP}/k_{cat,P} = (1/k_{-3})[1 + (k_3/k_{-2})(1 + k_2/k_{-1})] \quad (2d)$$

The steady state implies that the binding steps at the catalytic site are assumed to be faster than the rate of change of the surface composition. Often, enzyme kinetics are investigated under initial velocity conditions such that the concentration of the substrate can be considered constant. However, for the small systems described here, surface compositions can change very fast, as discussed above, and it is important to consider the time-dependent variation of substrate and product. Thus, in contrast to a true steady-state description, in the following the surface composition will be allowed to vary in the course of the catalytic action of the enzyme; this is sometimes referred to as a quasi-steady-state.

If both the products stay in the surface, the time-dependent change in surface composition due to the reaction leads to the differential equation

$$dX_P/dt = -dX_S/dt = v(t)/N_T \quad (3)$$

where $v(t)$ is given by v of eq 1 with X_S and X_P replaced by the time-dependent mole fractions $X_S(t)$ and $X_P(t)$. N_T is the total number of molecules (substrate, product, and inhibitor) in the outer surface of the vesicle. Furthermore, if all molecules remain in the surface it must hold that

$$X_P(t) = 1 - X_I - X_S(t) \quad (4)$$

This relation is based on the scheme in Figure 1 where each substrate molecule is turned into one product molecule. If the reaction results in two product molecules or more for each substrate, X_P should be interpreted as the mole fraction of substrate that has turned into product.

With eqs 1 and 4, eq 3 can be integrated to give an expression for the time-dependent change in product mole fraction. If the reaction starts with no product present [i.e., $X_P(0) = 0$, and consequently $X_S(0) = 1 - X_I$], the result can be expressed as

$$t = -(1/k_i)\ln[1 - X_P(t)/X_P(\infty)] + X_P(t)[N_T/v_0 - 1/k_iX_P(\infty)] \quad (5)$$

where $X_P(\infty) = (1 - X_I)/[1 + (K_{MS}k_{cat,P}/K_{MP}k_{cat,S})]$ is the equilibrium mole fraction product that is reached at the end of the reaction. When the logarithmic term dominates the right-hand side in eq 5, the reaction can be described as first order with an exponential relaxation rate k_i given by

$$\frac{1}{k_iN_T} = \frac{1 + X_I/K_I}{k_{cat,S}/K_{MS} + k_{cat,P}/K_{MP}} + \frac{(1 - X_I)(k_{cat,P} + k_{cat,S})}{K_{MS}K_{MP}(k_{cat,S}/K_{MS} + k_{cat,P}/K_{MP})^2} \quad (6)$$

The initial rate v_0 is given by eq 1 with $X_P = 0$ and $X_S = 1 - X_I$:

$$1/v_0 = (K_{MS}/k_{cat,S})[(1 + 1/K_I)X_I/(1 - X_I) + 1 + 1/K_{MS}] \quad (7)$$

Equation 5 is the general integrated Michaelis–Menten equation for a reversible catalysis on the surface in the presence of a competitive inhibitor. In the following we shall consider the irreversible limit where the backward reaction is zero, i.e., $k_{-2} = 0$. This is verified for the action of PLA2 on vesicles in the second paper in this series (Ghomashchi et al., 1990). Then $k_{cat,P} = 0$ so that we can call $k_{cat,S}$ simply k_{cat}, and K_{MP} becomes a dissociation constant for product, K_P ($K_P = k_3/k_{-3}$ in the scheme in Figure 1). This considerably simplifies the expressions above such that $X_P(\infty) = X_S(0) = 1 - X_I$. Introducing the total number, N_S, of substrate molecules initially in the outer surface of the vesicle

$$N_S = N_T(1 - X_I) \quad (8)$$

one finds from eq 5 that

$$t = -(1/k_i)\ln[1 - X_P(t)/(1 - X_I)] + N_S(1/v_0 - 1/k_iN_S)X_P(t)/(1 - X_I) \quad (9)$$

with exponential relaxation rate k_i determined by

$$1/k_iN_S = (K_{MS}/k_{cat})[(1 + 1/K_I)X_I/(1 - X_I) + 1 + 1/K_P] \quad (10)$$

and the initial rate v_0 as given by eq 7.

It should be noted that studying the whole reaction progress with decreasing substrate concentrations as in eq 9 corresponds to measuring initial rates at every intermediate surface composition. The initial rate v_0 from eq 7 is at high substrate levels, while k_iN_S is dominated by low substrate and high product levels. Equations 7, 9 and 10 form the basis for the kinetic study of PLA2. They were derived under the following assumptions: (i) one enzyme on the vesicle; (ii) no exchange of any molecules (enzyme, substrate, or products) between vesicles; (iii) irreversible product formation and no product present initially; (iv) steady-state approximation where the binding steps at the catalytic site are assumed to be much faster than the change in surface composition due to the reaction; (v) the intrinsic rate constants are independent of surface composition; (vi) components are mixed on the surface

and are not segregated; (vii) individual molecules of the various species occupy surface areas of similar size.

Some complications arising when requirements (i), (ii), or (vi) are not satisfied have been discussed previously (Jain & Berg, 1989). If (vii) does not hold so that individual molecules of the different species (substrate, product, and inhibitor) occupy surface areas of very dissimilar size, association rates to the enzyme may no longer be proportional to the mole fraction but instead proportional to the number of molecules per unit surface area (cf. Ransac et al., 1990). In this case, the fundamental rate constants k_1 and k_{-3} would be expressed in units of 1/(surface area)(time). Similarly, the derived constants (from eq 2a–d) K_{MS}, K_P, and K_I should be expressed in units of surface area. Analyzing the enzyme kinetics for this case in the same way as above, one finds that the resulting kinetic equation (eq 9) still holds but that the expressions for k_i and v_0, eqs 7 and 10, are different: In these two expressions, $1 + 1/K_I$ should be replaced by $A_I + 1/K_I$, $1 + 1/K_P$ by $A_P + 1/K_P$, and $1 + 1/K_{MS}$ by $A_S + 1/K_{MS}$, where A_S, A_P, and A_I denote the surface area of a molecule of substrate, product, or inhibitor, respectively. The same replacements would then also have to be carried out wherever possible in all the equations derived below. However, there exist also other possibilities to describe the kinetics if the molecules are dissimilar in surface area and there are no data to test these alternatives. This case will not be considered further below largely because the molecular areas of the substrate, both the products in a 1:1 mole ratio, and inhibitors used in the present study are comparable.

(3) The Reaction Progress Curve

In a kinetic experiment, one does not study an individual vesicle, but rather the total product formation from all vesicles. The integrated kinetic equation gives an implicit relation from which the reaction progress can be described. The result is particularly simple when there is at most one enzyme per vesicle and there is not a large variation in the size of the vesicles. If the total enzyme amount is C_E, then the total amount of product formed after time t is

$$P_t = C_E N_T X_P(t) \tag{11a}$$

which approaches

$$P_{max} = C_E N_T (1 - X_I) = C_E N_S \tag{11b}$$

at the end of the reaction. Thus the reaction progress is given by the result above, eq 9, with $X_P(t)/(1 - X_I)$ replaced by P_t/P_{max}:

$$k_i t = -\ln (1 - P_t/P_{max}) + (k_i N_S/v_0 - 1)P_t/P_{max} \tag{12}$$

Here v_0 and $N_S k_i$ are still given by eqs 7 and 10, respectively, in terms of the one-vesicle–one-enzyme situation. The total amount of products formed per unit time initially is simply $v_0 C_E$.

By fitting the reaction progress curve P_t/P_{max} versus t to this equation, one can find the parameters k_i and v_0, while N_S is determined from P_{max}/C_E (eq 11b). Since the curve fitting can be carried out with only two parameters, there is not enough information in the reaction progress curve to determine all three Michaelis–Menten parameters k_{cat}, K_{MS}, and K_P separately.

(3a) First-Order vs Zero-Order. The reaction progress curve is a mixture of first-order and zero-order components (eq 12). Depending on the kinetic parameters and the vesicle size, one or the other of these components may be more easily measured experimentally. When the logarithmic term on the right-hand side of eq 12 dominates over the term that is linear in P_t, the reaction progress curve can be expressed as

$$P_t/P_{max} \approx 1 - \exp(-k_i t) \tag{13}$$

Use of this approximation will give a relative error δ in the estimate of P_t/P_{max} of

$$\delta = (k_i N_S/V_0 - 1)(1 - P_t/P_{max}) \tag{14}$$

Thus as long as $|k_i N_S/v_0 - 1| \ll 1$, the first-order approximation is valid over the entire time course. In the absence of inhibitor ($X_I = 0$), one finds from eqs 7 and 10

$$k_i N_S/v_0 = (1 + 1/K_{MS})/(1 + 1/K_P) \tag{15}$$

indicating that the first-order approximation requires both $K_{MS} \gg 1$ and $K_P \gg 1$, or $K_{MS} \approx K_P$.

Under some circumstances, it may be easier to measure the initial rate. The first part of the reaction progress curve is linear in t,

$$P_t/P_{max} \approx (v_0/N_S)t \tag{16}$$

for small t. This approximation gives rise to a relative error δ:

$$\delta = (1/2)(v_0/k_i N_S)(P/P_{max}) = (1/2)[(1 + 1/K_P)/(1 + 1/K_{MS})](P/P_{max}) \tag{17}$$

This will occur at time t_d given by

$$t_d = 2\delta N_S k_i N_S/v_0^2 \tag{18}$$

Since $k_i N_S$ and v_0 are both independent of the vesicle size N_S, t_d is proportional to N_s, and larger vesicles will extend the actual time for which the zero-order approximation eq 16 can be used.

(3b) Inhibition. Competitive inhibitors will influence the two kinetic terms of the reaction progress differently. The most convenient way of studying their effects is to compare the kinetics in their presence and absence. Let us denote the initial rate in the presence of inhibitor by $(v_0)^I$ (given by v_0 of eq 7); and in the absence by $(v_0)^0$ (given by v_0 with $X_I = 0$). Taking the ratio of these, one finds

$$(v_0)^0/(v_0)^I = 1 + [(1 + 1/K_I)/(1 + 1/K_{MS})][X_I/(1 - X_I)] \tag{19}$$

Similarly, one can take the ratio of $k_i N_S$ in the absence of competitor, $(k_i N_S)^0$, and in the presence, $(k_i N_S)^I$, which gives from eq 10

$$(k_i N_S)^0/(k_i N_S)^I = 1 + [(1 + 1/K_I)/(1 + 1/K_P)][X_I/(1 - X_I)] \tag{20}$$

There is a nice symmetry in these two results, while the effect of the inhibitor on the initial rate depends on the substrate K_M value, K_{MS}, the effect on the exponential relaxation depends on product competition, K_P.

These inhibition equations look a little different from the usual bulk relations (Segel, 1975). This is primarily because the initial substrate concentration, X_S, depends on the amount of inhibitor present, $X_S(0) = 1 - X_I$, since it has been assumed that only substrate and inhibitor are present initially. It would be much less straightforward to try to vary the inhibitor concentration at fixed substrate as is normally done for enzyme kinetics in the bulk. Furthermore, eq 20 involves the number of substrate molecules, N_S, rather than the total number of molecules, N_T, in the outer surface of the vesicle; this is in contrast to our previous use (Jain & Berg, 1989) and is preferable both because N_S is a more directly accessible quantity and also because it leads to better symmetry in the relations.

In the limit of a very weak competitor, $K_I \to \infty$, the equations above can be used to estimate K_{MS} and K_P. In this limit,

the competitor is actually a neutral diluent. The variation of the amount of a neutral diluent in the surface would correspond to the variation of substrate concentration in the usual bulk kinetics. This is required for a complete kinetic analysis to find k_{cat}, K_{MS}, K_P, and the K_I's for various inhibitors.

K_I for a certain inhibitor can be determined from either eq 19 or eq 20 depending on which kind of measurement is most convenient and also which of K_{MS} and K_P is best known. As a control, K_I can be determined in both ways and should, of course, be the same. However, if $[X_I(50)]$ and $[n_I(50)]$ denote the mole fraction of inhibitor that reduces v_0 and k_iN_S, respectively, by 50%, one finds from eqs 19 and 20 that these two estimates of inhibitor strength will be different. This is related to the fact that a competitive inhibitor influences only the apparent K_M and not k_{cat}. Since v_0 is measured at a high substrate mole fraction and in the absence of product, while k_iN_S is dominated by low substrate and high product levels, the apparent K_M will be different. From eqs 19 and 20, the following relation for $[X_I(50)]$ and $[n_I(50)]$ can be derived:

$$\frac{1/[X_I(50)] - 1}{1/[n_I(50)] - 1} = \frac{1 + 1/K_P}{1 + 1/K_{MS}} \tag{21}$$

Thus, this relation should hold and be the same for all competitive inhibitors in the same substrate environment (see also eq 15). Consequently, the relation (eq 21) can serve as a control that indeed one is dealing with a competitive inhibitor.

(3c) Polydispersity in Vesicle Sizes. Small vesicles will have a faster depletion of available substrate on the surface than larger ones. Thus enzymes bound to vesicles of different sizes will see different environments and give different reaction progress curves. To account for the overall product production in the case where there is a large variation in size between different vesicles, one must take the proper averages.

Let us denote by $X_P(N,t)$ the mole fraction of product produced after time t on a vesicle that initially had N substrate molecules on its outer surface. Then $X_P(N,t)$ is determined by eq 9 with N_S replaced by N. The overall product production in the absence of inhibitor (i.e., $X_I = 0$) can be expressed as

$$P_t = \langle NX_P(N,t)\rangle C_E \tag{22}$$

with a maximum of

$$P_{max} = \langle N\rangle C_E \tag{23}$$

where $\langle\,\rangle$ denotes the proper statistical average over the vesicle size distribution. From eq 23, the average vesicle size can be calculated from the final level of total product production. The initial rate on a vesicle of size N is determined by

$$X_P(N,t) \approx (v_0/N)t \tag{24a}$$

for small t such that the total amount of product produced initially is from eq 22

$$P_t \approx v_0C_Et \tag{24b}$$

for small t and is independent of vesicle size distribution. Thus,

$$P_t/P_{max} \approx (v_0/\langle N\rangle)t \tag{25}$$

for small t such that initially the reaction progress P_t/P_{max} behaves as if all vesicles were of average size $\langle N\rangle$.

When the first-order reaction dominates, one has

$$X_P(N,t) \approx 1 - \exp[-k_i(N)t] \tag{26}$$

$k_i(N)$ is the exponential relaxation rate for a vesicle of size N and is proportional to $1/N$, as given in eq 10. Thus, in this limit one finds from eq 22

$$P_t \approx C_E\{\langle N\rangle - \langle N\exp[-k_i(N)t]\rangle\} \tag{27}$$

To calculate the second average, we shall use the general approximation for the average of a function of a variable x over a distribution of x values with an average $\langle x\rangle$ and variance σ^2:

$$\langle F(x)\rangle \approx F(\langle x\rangle) + (1/2)\sigma^2F''(\langle x\rangle) \tag{28}$$

For eq 27 this approximation gives

$$P_t/P_{max} \approx 1 - [1 + 0.5\sigma^2_{rel}(k_it)^2]\exp(-k_it) \tag{29}$$

In this expression, $k_i = k_i(\langle N\rangle)$ is the exponential relaxation rate for a vesicle of average size $\langle N\rangle$ and $\sigma^2_{rel} = \sigma^2/\langle N\rangle^2 = \langle(N - \langle N\rangle)^2\rangle/\langle N\rangle^2$ is the relative variance in the vesicle size distribution. The preexponential correction factor in eq 29 is the influence from the size distribution.

Thus a polydispersity in vesicle size influences primarily the approach to the final product level by slowing it down. Numerically, one finds that this distortion of the reaction progress curve is significant only when $\sigma^2_{rel} \approx 0.2$ or larger. This corresponds to a size distribution where most vesicles have N_S values within 45% of the average. Thus, a fairly large size variation is allowed without distorting the simple results. The calculations require, however, that there is not a significant tail of very small vesicles.

(3d) More than One Enzyme per Vesicle. Unless the enzyme-to-vesicle ratio is kept low, there will be a distribution of different number of enzymes on different vesicles. A vesicle with more than one enzyme bound will be depleted faster of available substrate than a vesicle with only one enzyme. Thus when there is a distribution of enzyme numbers, different enzymes will see different environments, and this must be accounted for when calculating the overall reaction progress curve.

Let us denote with $X_P(j,t)$ the mole fraction of product at time t on a vesicle with j enzymes bound. The rate of change of $X_P(j,t)$ will be j times faster than for the case with one enzyme. Thus (cf. eq 3),

$$dX_P(j,t)/dt = jv(t)(1 - X_I)/N_S \tag{30}$$

where $v(t)$ as given by eq 1 refers to the reaction velocity for one enzyme and is independent of j. As a consequence, $X_P(j,t) = X_P(1,jt) = X_P(jt)$, and the number of enzymes enters only as a rescaling of the time axis compared to the case for one enzyme, simply replacing t by jt. The overall reaction progress can be calculated by taking the appropriate averages over the number distribution.

If there is a random distribution of enzymes over different vesicles, the probability P_j that a vesicle has j enzymes will follow a Poissonian distribution:

$$P_j = J^j\exp(-J)/J! \tag{31}$$

$J = C_E/C_V$ is the ratio of enzyme-to-vesicle concentration that corresponds to the average number of enzymes per vesicle. The maximal amount of product formed is

$$P_{max} = N_SC_V[1 - \exp(-J)] \tag{32}$$

which approaches the relation given above (eq 12) only when $J \ll 1$. Thus if N_S is estimated as P_{max}/C_E, this will be a factor of $J/[1 - \exp(-J)]$ smaller than the real value for the vesicle size. This would lead to an underestimate of N_S by 21% for $J = 0.5$ and by 14% for $J = 0.3$.

The overall product formation will be given by the average over all vesicles:

$$P_t = N_TC_V\sum_{j=1}^{\infty}P_jX_P(j,t) \tag{33}$$

which at short times gives

$$P_t \approx C_Ev_0t \tag{34}$$

for small t. Thus the initial rate is independent of the enzyme distribution, as could be expected, and the kinetic parameter v_0 can be estimated directly from the initial slope of P_t. The initial slope of the reaction progress curve, P_t/P_{max}, however, will depend on the enzyme-to-vesicle ratio $J = C_E/C_V$ as

$$P_t/P_{max} \approx \{J/[1 - \exp(-J)]\}(v_0/N_S)t \quad (35)$$

for small t.

In the limit where the exponential relaxation dominates, one finds from eq 33 that

$$P_t \approx C_V N_S[1 - \exp[-J[1 - \exp(-k_i t)]]] \quad (36)$$

as before (Jain & Berg, 1989). Taking the ratio P_t/P_{max} from eqs 36 and 32 and trying to fit that to the simple relation in eq 13 would lead to an overestimate of the relaxation rate k_i by ca. 30% if $J = 1$ and by ca. 15% for $J = 0.5$. The enzyme-to-vesicle ratio J should be smaller than $J \approx 0.3$ for a smaller than 10% error in the k_i estimate based on curve fitting with the one-vesicle-per-enzyme relations.

In the other limit when J is large ($J > 10$ or so), the small-number fluctuations in the number of enzymes per vesicle become negligible and eq 36 approaches the limit

$$P_t = C_V N_S[1 - \exp(-Jk_i t)] \quad (37)$$

Thus in this limit of a large enzyme-to-vesicle ratio, the reaction will proceed as though every vesicle carries the average number, J, of enzymes, and the reaction progress curve will again approach that given by eq 12 with k_i replaced by Jk_i and N_S replaced by N_S/J.

This discussion assumes that N_S denotes the number of substrates initially in the outer surface of a vesicle as defined above from the one-vesicle-per-enzyme case. However, when there are more than one enzyme per vesicle, it would be more convenient to use $N_S = P_{max}/C_E$ as a definition and define k_i from eq 10. In this way the reaction progress curve would be described by eq 12 both at small ($J \ll 1$) and large ($J \gg 1$) enzyme-to-vesicle ratios. As discussed above, complications arise at intermediate values of J.

(4) Substrate Specificity

The substrate specificity of the enzyme can be studied in a system where there are two different kinds of substrates available in the surface. In the reaction scheme, the steady-state rate of product production per enzyme at any particular time can be expressed as

$$v = [k_1 k_2/(k_{-1} + k_2)]X_S E_f = (k_{cat}/K_{MS})X_S E_f \quad (38)$$

where X_S is the mole fraction of the substrate under consideration that is available in the interface and E_f is the probability that an enzyme bound at the interface has its catalytic site free. Thus eq 38 is the steady-state equation for the velocity in terms of the free enzyme in the interface (E*) rather than the total enzyme (free + complexed, i.e., E* + E*S) in the interface as in eq 7 (Fersht, 1985). In general E_f will be a function of the composition of the surface that can give rise to a complicated reaction progress curve; fortunately, as shown below, this is of no consequence in the study of specificity. If the number of product molecules produced by the enzyme after time t is $N_P(t)$, the rate of production is v and

$$dN_P/dt = v \quad (39)$$

Furthermore, if there is no product present initially, the number of product molecules produced until the end of the reaction, $N_P(\infty)$, is the same as the number of substrate molecules available initially, and the mole fraction of substrate remaining in the surface at time t can be expressed as

$$X_S(t) = [N_P(\infty) - N_P(t)]/N_T \quad (40)$$

where N_T is the total number of molecules (substrate, product, inhibitor, etc.) in the outer surface of a vesicle. Equations 38–40 can be integrated directly to give

$$\ln [1 - N_P(t)/N_P(\infty)] = -\int_0^t (1/N_T)(k_{cat}/K_{MS})E_f(t')dt' \quad (41)$$

These relations hold at either small ($J \ll 1$) or large ($J \gg 1$) enzyme-to-vesicle ratios, and they are valid regardless of the presence in the interface of inhibitors or competing substrates; such competition effects are included in the factor $E_f(t)$. If all enzymes have the same "history", there will be no difference in the integral over E_f for different enzymes or different vesicles. This will be the case if all vesicles are the same initially, if there is at most one enzyme per vesicle, and if there is no intervesicle exchange of enzyme molecules. (Alternatively, all enzymes would have the same "history" also in the limit where there are many more than one enzyme for every vesicle.) Thus, if these conditions hold, one gets the following simple ratio for two competing substrates that yield products P1 and P2, respectively:

$$\frac{\ln [1 - N_{P1}(t)/N_{P1}(\infty)]}{\ln [1 - N_{P2}(t)/N_{P2}(\infty)]} = \frac{(k_{cat}/K_{MS})_1}{(k_{cat}/K_{MS})_2} \quad (42)$$

Thus by comparing the reaction progress for two different substrates in this way, one gets a ratio of the kinetic parameter combination $k_{cat}/K_{MS} = k_2/(k_{-1} + k_2)$ for the two substrates. This provides information on the specificity of the enzyme for these substrates.

(5) Conclusions

Interfacial catalysis in the scooting mode can be analyzed with a straightforward generalization of the usual methods of enzyme kinetics. Due to the special constraints of the structured surface, the resulting equations become somewhat different. The definitions and calculations above are based on the one-vesicle-per-enzyme case since this has been experimentally most accessible. The limits of validity of the description have been explored by considering some departures from the simple limit. Furthermore, in a previous communication (Jain & Berg, 1989), we have described some of the complications that appear when the enzyme is not operating in the scooting mode.

References

Apitz-Castro, R. J., Jain, M. K., & de Haas, G. H. (1982) *Biochim. Biophys. Acta 688*, 349–356.

Bonsen, P. P. M., de Haas, G. H., Pieterson, W. A., & van Deenen, L. L. M. (1972) *Biochim. Biophys. Acta 270*, 264–282.

Burch, R. M. (1989) *Mol. Neurobiol. 3*, 155–171.

Cevc, G., & Marsh, D. (1987) *Phospholipid Bilayers*, Wiley, New York.

de Haas, G. H., Bonsen, P. P. M., Pieterson, W. A., & van Deenen, L. L. M. (1971) *Biochim. Biophys. Acta 239*, 252–266.

de Haas, G. H., Dijkman, R., van Oort, M. G., & Verger, R. (1990) *Biochim. Biophys. Acta 1043*, 75–82.

Dennis, E. A. (1973a) *J. Lipid Res. 14*, 152–159.

Dennis, E. A. (1973b) *Arch. Biochem. Biophys. 158*, 485–493.

Dennis, E. A. (1983) in *The Enzymes*, Vol. *16*, pp 307–353, Academic Press, New York.

Donne-op den Kelder, G. M., de Haas, G. H., & Egmond, M. R. (1983) *Biochemistry 22*, 2470–2478.

Fersht, A. (1985) *Enzyme Structure and Mechanism*, W. H. Freeman & Co., San Francisco, CA.
Fleer, E. A. M., Verheij, H. M., & de Haas, G. H. (1981) *Eur. J. Biochem. 113*, 283–288.
Gallin, J. I., Goldstein, I. M., & Snyderman, R., Eds. (1988) *Inflammation*, Raven Press, New York.
Ghomashchi, F., O'Hare, T., Clary, D., & Gelb, M. H. (1991a) *Biochemistry 30* (second paper of six in this issue).
Ghomashchi, F., Yu, B. Z., Berg, O., Jain, M. K., & Gelb, M. H. (1991b) *Biochemistry 30* (fourth paper of six in this issue).
Gratzer, W. B., & Beaven, G. H. (1977) *Methods Enzymol. 81*, 118–129.
Irvine, R. F. (1982) *Biochem. J. 204*, 3–8.
Jain, M. K. (1972) *Curr. Top. Membr. Transp. 4*, 175–254.
Jain, M. K. (1988) *Introduction to Biomembranes*, p 423, Wiley, New York.
Jain, M. K., & Cordes, E. H. (1973a) *J. Membr. Biol. 14*, 101.
Jain, M. K., & Cordes, E. H. (1973b) *J. Membr. Biol. 14*, 119.
Jain, M. K., & Jahagirdar, D. V. (1985a) *Biochim. Biophys. Acta 814*, 313–318.
Jain, M. K., & Jahagirdar, D. V. (1985b) *Biochim. Biophys. Acta 814*, 319–326.
Jain, M. K., & Berg, O. G. (1989) *Biochim. Biophys. Acta 1002*, 127–156.
Jain, M. K., & Rogers, J. (1989) *Biochim. Biophys. Acta 1003*, 91–97.
Jain, M. K., & Gelb, M. H. (1991) *Methods Enzymol.* 197, 112–125.
Jain, M. K., Egmond, M. R., Verheij, H. M., Apitz-Castro, R. J., Dijkman, R., & de Haas, G. H. (1982) *Biochim. Biophys. Acta 688*, 341–348.
Jain, M. K., Rogers, J., Jahagirdar, D. V., Marecek, J. F., & Ramirez, F. (1986a) *Biochim. Biophys. Acta 860*, 435–447.
Jain, M. K., Maliwal, B. P., de Haas, G. H., & Slotboom, A. J. (1986b) *Biochim. Biophys. Acta 860*, 448–461.
Jain, M. K., Rogers, J., Marecek, J. F., Ramirez, F., & Eibl, H. (1986c) *Biochim. Biophys. Acta 860*, 462–474.
Jain, M. K., de Haas, G. H., Marecek, J. F., & Ramirez, F. (1986d) *Biochim. Biophys. Acta 860*, 475–483.
Jain, M. K., Rogers, J., & de Haas, G. H. (1988) *Biochim. Biophys. Acta 940*, 51–62.
Jain, M. K., Yuan, W., & Gelb, M. H. (1989a) *Biochemistry 28*, 4135–4139.
Jain, M. K., Yu, B.-Z., & Kozubek, A. (1989b) *Biochim. Biophys. Acta 980*, 23–32.
Jain, M. K., Yu, B.-Z., Rogers, J., Ranadive, G. N., & Berg, O. G. (1991a) *Biochemistry 30* (third paper of six in this issue).
Jain, M. K., Ranadive, G. N., Yu, B.-Z., & Verheij, H. M. (1991b) *Biochemistry 30* (fifth paper of six in this issue).
Jain, M. K., Rogers, J., Berg, O. & Gelb, M. H. (1991c) *Biochemistry 30* (sixth paper of six in this issue).
Jencks, W. (1969) *Catalysis in Chemistry and Enzymology*, McGraw Hill, New York.
Nayar, R., Hope, M. J., & Cullis, P. R. (1989) *Biochim. Biophys. Acta 986*, 200–206.
Nichols, J. W. (1988) *Biochemistry 27*, 3925–3931.
Nichols, J. W., & Ozarowska, J. (1990) *Biochemistry 29*, 4600–4606.
Niewenhuizen, W., Kunze, H., & de Haas, G. H. (1974) *Methods Enzymol. 32B*, 147–154.
Nir, S., Bentz, J., Wilshut, J., & Duzgunes, N. (1983) *Prog. Surf. Sci. 13*, 1–124.
Papahadjopoulos, D., & Kimelberg, J. K. (1975) *Prog. Surf. Sci. 4*, 141–232.
Pattus, F., Slotboom, A. J., & de Haas, G. H. (1979) *Biochemistry 18*, 2698–2702.
Pieterson, W. A., Volwerk, J. J., & de Haas, G. H. (1974a) *Biochemistry 13*, 1439–1445.
Pieterson, W. A., Vidal, J. C., Volwerk, J. J., & de Haas, G. H. (1974b) *Biochemistry 13*, 1455–60.
Ransac, S., Riviere, C., Soulie, J. M., Gancet, C., Verger, R., & de Haas, G. H. (1990) *Biochim. Biophys. Acta 1043*, 57–66.
Segel, I. H., (1975) *Enzyme Kinetics*, Wiley, New York.
Slotboom, A. J., Jensen, E. H. J. M., Vlijm, H., Pattus, F., Soares de Araujo, P., & de Haas, G. H. (1978) *Biochemistry 17*, 4593–4600.
Szoka, F., & Papahadjopoulos, D. (1980) *Annu. Rev. Biophys. Bioeng. 9*, 467–508.
van den Bergh, C. J., Bekkers, A. C. A. P. A., Verheij, H. M., & de Haas, G. H. (1989) *Eur. J. Biochem. 182*, 307–313.
van Oort, M. G., Dijkman, R., Hille, J. D. R., & de Haas, G. H. (1985) *Biochemistry 24*, 7987–7993.
Verger, R., & de Haas, G. H. (1973) *Chem. Phys. Lipids 10*, 127–136.
Verger, R., & de Haas, G. H. (1976) *Annu. Rev. Biophys. Bioeng. 5*, 77–117.
Verheij, H. M., Volwerk, J. J., Jansen, E. H. J. M., Puijk, W. C., Dijkstra, B. W., Drenth, J., & de Haas, G. H. (1980) *Biochemistry 19*, 743–750.
Verheij, H. M., Slotboom, A. J., & de Haas, G. H. (1981) *Rev. Physiol., Biochem. Pharmacol. 91*, 91–203.